Crack Propagation Path in Two-Directionally Graded Composites Subjected to Mixed-Mode I+II Loading

Zhao Zhenbo, *Xu Xiwu**, *Guo Shuxiang*

State Key Laboratory of Mechanics and Control of Mechanical Structures, Nanjing University of Aeronautics and Astronautics, Nanjing 210016, P. R. China

(Received 28 August 2016; revised 20 March 2017; accepted 28 April 2017)

Abstract: Crack propagation path in two-directionally graded composites was investigated by the finite element method. A graded extended finite element method (XFEM) was employed to calculate displacement and stress fields in cracked graded structures. And a post-processing subroutine of interaction energy integral was implemented to extract the mixed-mode stress intensity factors (SIFs). The maximum hoop stress (MHS) criterion was adopted to predict crack growth direction based on the assumption of local homogenization of asymptotic crack-tip fields in graded materials. Effects of material nonhomogeneous parameters on crack propagation paths were also discussed in detail. It is shown that the present method can provide relatively accurate predictions of crack paths in two-directionally graded composites. Crack propagates in the decreasing direction of effective Young′s modulus. The shape and steepness of property gradient perpendicular to the crack surface have great influences on crack paths. Through redesigning material property reasonably, crack growth in graded material can be changed to improve mechanical behaviours of cracked structures.

Key words: crack propagation; two-directionally graded composites; extended finite element method(XFEM); interaction integral

CLC number: TB333; O342 **Document code**: A **Article ID**: 1005-1120(2017)03-0272-14

0 Introduction

Traditional unidirectionally graded composites (or functionally graded materials, FGMs) have been used in several of industry applications because of their excellent thermal stress relaxation capability for structures serving in thermal environments. Two-directionally graded composites (2D-GCs or two-directionally functionally graded materials, 2D-FGMs) are a new kind of advanced inhomogeneous composites in which the constituent volume fractions and effective thermal-mechanical properties vary smoothly in two directions. For structures serving in severe temperature environments, 2D-GCs have more excellent thermal stress reduction capability and flexible designable structures than those of FGM. Therefore, 2D-GCs have received increasingly attentions in research and practice[1].

Initiation, propagation and coalescence of micro-cracks are the most important failure mechanisms for engineering structures, especially for graded structures serving in severe thermal gradient conditions. Therefore, fracture mechanics of graded composites has been studied extensively in order to understand the relationship between property gradients and crack behaviors.

Nemat-Alla and Noda[2-3] studied the edge crack problems in semi-infinite nonhomogeneous materials with bi-directionally varying coefficient of thermal expansion under thermal loadings by singular integral equation method. However, the materials considered in Refs. [2—3] are not realistic 2D-GCs because the Young′s modulus, Poisson ratio and thermal conductivity were all assumed to vary in one direction. Nemat-Alla et

* Corresponding author, E-mail address: xwxu@nuaa.edu.cn.

How to cite this article: Zhao Zhenbo, Xu Xiwu, Guo Shuxiang. Crack propagation path in two-directionally graded composites subjected to mixed-mode I+II loading[J]. Trans. Nanjing Univ. Aero. Astro., 2017,34(3):272-285.
http://dx.doi.org/10.16356/j.1005-1120.2017.03.272

al.[4-5] firstly proposed the factual 2D-GCs whose thermal-mechanical properties were all changed in two directions. In their work, the composites were constituted by one ceramic and two metal components and the macro-properties were predicted by modified rules of mixture. The steady thermal-elastic and transient thermal-plastic responses of 2D-FGMs under non-uniform thermal loadings were studied by finite element method and the more excellent thermal stress reduction characteristics in 2D-FGMs were validated. Thereafter, Nemat-Alla[6] further studied the composition optimization problem for ZrO_2/6061-T6/Ti-6Al-4V 2D-FGMs under severe thermal cycles by elastic-plastic finite element method based on the minimum peak temperature criterion and minimum thermal stress criterion. Asgari and Akhlaghi[7-8] analyzed the transient heat conduction and thermal stress problems in two-directionally graded thick hollow cylinder with finite length. Effects of variation of material components in radial and axial directions on temperature and thermal stress fields were discussed and the results showed that more flexible structures can be achieved to fulfill various design requirements by using 2D-GCs. Sakurai[9] investigated the transient and steady-state heat conductions of 2D-FGMs by particle method. Asgari et al.[10] conducted the dynamic analysis of two-directionally graded thick hollow cylinder under impact loading by finite element method. Asemi et al.[11] proposed the elastic solutions of two-directionally graded thick truncated cone with finite length under hydrostatic combined loads. Torshizian et al.[12] calculated mode-III stress intensity factors (SIFs) for an arbitrary oriented crack in 2D-FGMs by using singular integral equation and finite element method. Torshizian et al. concluded that the mode-III SIFs have higher values when material parameters vary parallel to the crack surface and mode-III SIFs in 2D-FGMs are always greater than those in traditional one-directionally graded composites. Torshizian et al.[13] then calculated mix-mode SIFs at the arbitrarily oriented crack tips under in-plane mechanical loads in 2D-GCs and the effects of crack orientation and material non-homogeneity on SIF have been discussed. Some other studies on SIFs in two-directionally graded materials can be found in Chen et al.[14] However, according to the authors' knowledge, there have not been detailed studied on the crack propagation paths in 2D-GCs. We investigated three issues: (1) The calculation capacity of graded extended finite element is demonstrated; (2) crack propagation paths in 2D-GCs are simulated; (3) the rationality of maximum hoop stress (MHS) criterion and local homogenization hypothesis at crack-tip is discussed for crack propagation simulation in graded composites.

1 Constituent Volume Fractions and Effective Properties

As in Ref. [5], the 2D-GCs are constituted by three distinctive components with varying volume fractions in two directions. Consider a two-directionally graded rectangular plate of width W and height h as shown in Fig. 1. The composition at the upper surface ($y=h$) is constituent 3, and the material at the bottom surface ($y=0$) changes from constituent 1 at the left corner ($x=0$) to constituent 2 at the right corner ($x=W$). Accordingly, the constituent volume fraction distributions at point A are expressed as

$$V_1(x,y)=\left[1-\left(\frac{y}{h}\right)^{m_y}\right]\cdot\left[1-\left(\frac{x}{W}\right)^{m_x}\right] \quad (1)$$

$$V_2(x,y)=\left[1-\left(\frac{y}{h}\right)^{m_y}\right]\cdot\left(\frac{x}{W}\right)^{m_x} \quad (2)$$

$$V_3(x,y)=\left(\frac{y}{h}\right)^{m_y} \quad (3)$$

where V_1, V_2 and V_3 are the volume fractions of the three constituents; m_x and m_y the nonhomogeneous parameters which describe the composition variations of 2D-GCs in x and y directions, respectively; W and h the width and the height of two-directionally graded plate as shown in Fig. 1. Obviously, 2D-GCs degenerate to traditional homogeneous materials (constituent 3) when $m_x=m_y=0$.

Traditional micromechanical models, including Mori-Tanaka method, self-consistent meth-

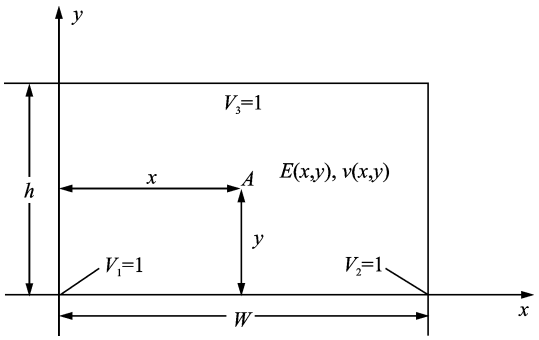

Fig. 1 Geometrical dimensions and constituents of two-directionally graded plate

od and three phase model, can be utilized to predict the effective properties of graded composites and can therefore achieve relatively accurate results in practice[15]. In this paper, Mori-Tanaka method is adopted to predict the effective mechanical parameters of 2D-GCs and the properties can be expressed as

$$\kappa^e = \frac{\sum_{i=1}^{3} \frac{V_i \kappa_i}{3\kappa_i + 4\mu_1}}{\sum_{i=1}^{3} \frac{V_i}{3\kappa_i + 4\mu_1}} \tag{4}$$

$$\mu^e = \mu_1 \frac{\sum_{i=2}^{3} \frac{V_i \mu_i}{(7-5\nu_1)\mu_1 + (8-10\nu_1)\mu_i} + \frac{V_1}{15(1-\nu_1)}}{\sum_{i=2}^{3} \frac{V_i \mu_1}{(7-5\nu_1)\mu_1 + (8-10\nu_1)\mu_i} + \frac{V_1}{15(1-\nu_1)}} \tag{5}$$

$$E^e = \frac{9\kappa^e \mu^e}{\mu^e + 3\kappa^e}, \nu^e = \frac{3\kappa^e - 2\mu^e}{2(\mu^e + 3\kappa^e)} \tag{6}$$

where κ^e, μ^e, E^e and ν^e are the effective bulk modulus, the shear modulus, the Young's modulus and the Poisson's ratio, respectively; κ_i, μ_i and V_i the bulk modulus, the shear modulus and the volume fractions of component i, respectively; and ν_1 is the Poisson's ratio of constituent 1. Through altering the volume fractions of constituent 1—3, spatially varying mechanical properties in x and y directions can be realized in 2D-GCs. Assuming $m_x = m_y = 1.0$, which means the volume fractions vary linearly, the effective Young's modulus and the Poisson's ratio are shown in Fig. 2 (see details in section 5.2). It can be seen that 2D-GCs have bi-directional property variations in both x and y directions.

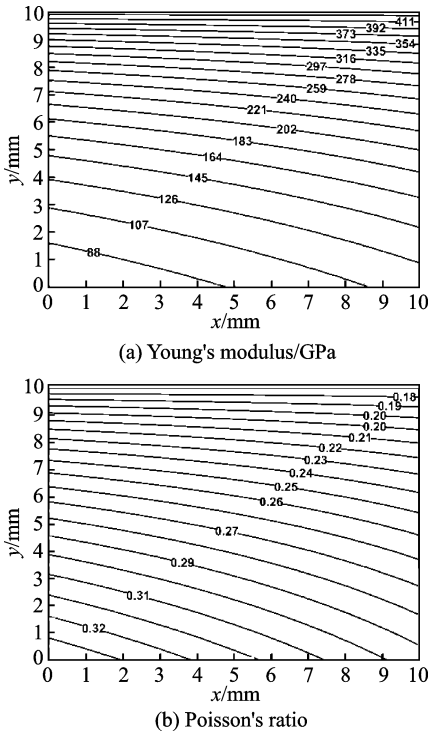

Fig. 2 Effective property distribution in two-directionally graded composites

2 Constituent Volume Fractions and Effective Properties

In extended finite element method (XFEM), traditional displacement approximation is enriched by discontinuous and crack-tip asymptotic fields which are used to describe the displacement discontinuity across crack faces and stress singularity at crack tips, respectively[16]. By this technique, cracks can be represented independently from mesh topology and remeshing is not needed during crack propagations. More details about XFEM can be found in Ref. [17]. The general theory framework about graded XFEM is introduced as below.

Considering a linear elastic and isotropic cracked body, and assuming small deformation and traction-free crack surfaces, the weak form of equilibrium equations can be expressed as

$$\int_\Omega \boldsymbol{\sigma}(x) : \delta\boldsymbol{\varepsilon} \, \mathrm{d}\Omega = \int_\Omega \boldsymbol{b} \cdot \delta\boldsymbol{u} \, \mathrm{d}\Omega + \int_{\Gamma_t} \bar{\boldsymbol{t}} \cdot \delta\boldsymbol{u} \, \mathrm{d}\Gamma \tag{7}$$

where Ω is the volume domain and Γ the traction boundary; $\boldsymbol{b}$ and $\bar{\boldsymbol{t}}$ are the body force per unit vol-

ume and prescribed boundary traction, respectively; $\boldsymbol{\sigma}(x)$ is the Cauchy stress tensor holding the relationship $\boldsymbol{\sigma}(x)=\boldsymbol{C}(x):\boldsymbol{\varepsilon}(\boldsymbol{u})$ where $\boldsymbol{C}(x)$ is the constitutive tensor of 2D-GCs, $\boldsymbol{\varepsilon}$ the strain tensor and $\boldsymbol{u}$ the trial displacement vector. $\delta\boldsymbol{u}$ and $\delta\boldsymbol{\varepsilon}$ are virtual displacement vector and strain tensor (test function space), respectively. Substituting the constitutive relationship into Eq. (7), one can obtain the following integral equation

$$\int_{\Omega}\boldsymbol{\varepsilon}^{\mathrm{T}}:\boldsymbol{C}(x):\delta\boldsymbol{\varepsilon}\,\mathrm{d}\Omega=\int_{\Omega}\boldsymbol{b}\cdot\delta\boldsymbol{u}\,\mathrm{d}\Omega+\int_{\Gamma_t}\bar{\boldsymbol{t}}\cdot\delta\boldsymbol{u}\,\mathrm{d}\Gamma \tag{8}$$

In XFEM, the enriched trial and test displacement fields are both expressed as in Ref. [16]

$$\boldsymbol{u}(x)=\sum_{I\in\boldsymbol{N}}N_I(x)\boldsymbol{u}_I+\sum_{I\in\boldsymbol{N}_\Gamma}N_I(x)H_I(x)\boldsymbol{a}_I+\sum_{I\in\boldsymbol{N}_\Lambda}N_I(x)\Big[\sum_{\alpha=1}^{4}\Phi_I^{\alpha}(x)\boldsymbol{b}_I^{\alpha}\Big] \tag{9}$$

where $N_I(x)$, $H_I(x)$ and $\Phi_I^{\alpha}(x)$ are the traditional displacement interpolation function, Heaviside function and crack-tip asymptotic functions, respectively; $\boldsymbol{u}_I$ is the continuous displacement vector; $\boldsymbol{a}_I$ is the enriched degree of freedom vector associated with Heaviside function; and $\boldsymbol{b}_I^{\alpha}$ the enriched degree of freedom vectors associated with crack-tip asymptotic functions. N is the set of all nodes, N_Γ and N_Λ are the sets of nodes enriched by Heaviside function and crack-tip asymptotic functions, respectively. The selection of enriched nodes is shown in Fig. 3 where the circle and square dots are nodes enriched by Heaviside and crack-tip functions, respectively.

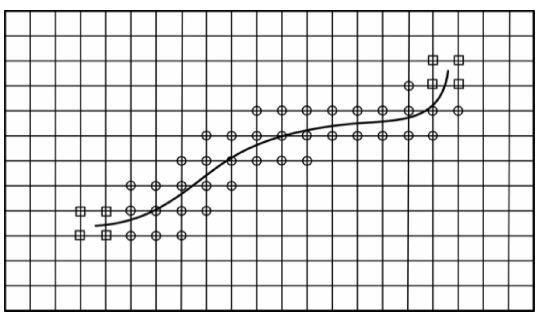

Fig. 3 Heaviside enriched nodes (circle dots) and crack-tip enriched nodes (square dots) in extended finite element method

A detailed selection algorithm is provided in Ref. [17]. In XFEM, Heaviside and crack-tip function enriched nodes are specified by setting $\boldsymbol{b}_I^{\alpha}=0$ ($\alpha=1$—4) and $\boldsymbol{a}_I=0$, respectively. And for other unenriched nodes, all the enriched degree of freedom vectors are setting as $\boldsymbol{a}_I=\boldsymbol{b}_I^{\alpha}=0$. For 4-node linear extended finite element with four Gauss points in linear elastic crack problem, expressions of $N_I(x)$, $H_I(x)$ and $\Phi_I^{\alpha}(x)$ are written as

$$N_I(x)=\frac{1}{4}(1+\xi_I\xi)(1+\eta_I\eta) \tag{10}$$

$$H_I(x)=\begin{cases}1 & \text{Above crack}\\ -1 & \text{Below crack}\end{cases} \tag{11}$$

$$\Phi_I^{\alpha}(x)=\sqrt{r}\cdot\left\{\sin\frac{\theta}{2},\cos\frac{\theta}{2},\sin\theta\sin\frac{\theta}{2},\sin\theta\cos\frac{\theta}{2}\right\} \tag{12}$$

where (ξ,η) is the Gauss coordinates and (r,θ) the polar coordinates at crack-tips.

Substituting Eq. (9) into Eq. (8) and considering the strain-displacement relationship, one can obtain the finite element equation system of graded XFEM

$$\boldsymbol{K}\boldsymbol{u}=\boldsymbol{f} \tag{13}$$

where $\boldsymbol{u}$ is the unknown extended nodal displacement vector, $\boldsymbol{K}$ and $\boldsymbol{f}$ are the global element stiffness matrix and nodal external force vector, respectively. The detailed expressions for $\boldsymbol{u}$ and $\boldsymbol{f}$ can be found in Ref. [17], and $\boldsymbol{K}$ is expressed at the element scale as

$$\boldsymbol{k}_{ij}^{e}=\begin{bmatrix}k_{ij}^{uu} & k_{ij}^{ua} & k_{ij}^{ub}\\ k_{ij}^{au} & k_{ij}^{aa} & k_{ij}^{ab}\\ k_{ij}^{bu} & k_{ij}^{ba} & k_{ij}^{bb}\end{bmatrix} \tag{14}$$

$$k_{ij}^{rs}(x)=\int_{\Omega^e}(B_i^r)^{\mathrm{T}}\boldsymbol{C}(x)B_j^s\,\mathrm{d}\Omega;r,s=u,a,b \tag{15}$$

where B_i^r are the derivative matrix of extended shape functions (including the standard shape functions and the products of standard shape functions and enriched functions) which can also be found in Ref. [17]. Note that $\boldsymbol{k}^e(x)$ in Eqs. (14, 15) is the spatially varying stiffness matrix of graded extended finite element and Gauss integral scheme is employed to calculate $\boldsymbol{k}^e(x)$ by substituting Young's modulus and Poisson's ratio at Gauss points (calculated by Eqs. (4)—(6)) in-

to constitutive tensor $\boldsymbol{C}(x)$. Kim and Paulino[18] have demonstrated that graded elements which embed property variations into element scale can provide more accurate local stress fields, which is considerably important for crack propagation path predictions in two-directionally graded materials.

In the present paper, graded XFEM is implemented and embedded into finite element software ABAQUS by user defined element UEL subroutine in the framework of FORTRAN. On the basis of the graded XFEM, a continuous graded finite element model is established to calculate stress/strain fields of cracked two-directionally graded structures. Furthermore, it is worthy to note that the realization of graded element stiffness matrix in the proposed graded XFEM is not limited to Mori-Tanaka method, and other micromechanical models and analytical expressions (e. g. , exponential functions or power functions) can also be adopted.

3 Extraction of Stress Intensity Factors and Crack Growth Direction

Based on the calculation results from graded XFEM, interaction energy integral is used here to extract mixed-mode SIFs and crack growth direction by introducing independent auxiliary displacement/stress fields. Considering traction-free crack surfaces, standard J_1 integral can be defined as in Ref. [19]

$$J_1 = \lim_{\Gamma_s \to 0} \oint_{\Gamma} (\sigma_{ij} u_{i,1} - W_e \delta_{1j}) \boldsymbol{m}_j q \, \mathrm{d}\Gamma \tag{16}$$

where $\Gamma = \Gamma_0 + \Gamma^+ - \Gamma_s + \Gamma^-$ is the integral path in Fig. 4; $\boldsymbol{m}_j$ the unit outward normal vector to contour Γ; $u_{i,1}$ the derivative of displacement u_i to crack-tip local coordinate x; W_e the elastic strain energy density; δ_{1j} the Kronecker symbol; q a weight function changing from unit at Γ_s to zero at Γ_0.

For convenient calculation from finite element solutions, J_1 can be recast into a domain integral form by applying the divergence theorem

$$J_1 = \int_{\Omega} (\sigma_{ij} u_{i,1} - W_e \delta_{1j}) q_{,j} \, \mathrm{d}\Omega + \int_{\Omega} (\sigma_{ij} u_{i,1} - W_e \delta_{1j})_{,j} q \, \mathrm{d}\Omega \tag{17}$$

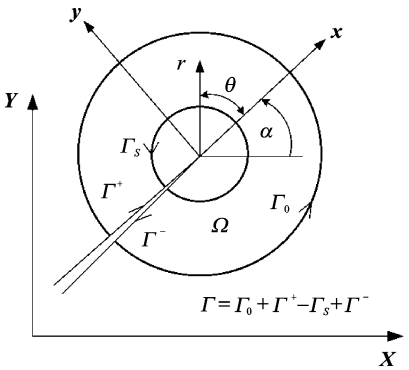

Fig. 4 Schematic diagram of contour integral path at crack-tip coordinate system

where Ω is the domain enclosed by contour Γ. Considering two independent fields of (u, σ, ε) and (u^{aux}, σ^{aux}, $\varepsilon^{\mathrm{aux}}$) which are the actual and auxiliary fields, respectively. Take the superimposed fields (summation of the actual and auxiliary fields) into Eq. (17) and after some algebraic derivations, interaction energy integral can be obtained

$$I = \int_{\Omega} (\sigma_{ij} u^{\mathrm{aux}}_{i,1} + \sigma^{\mathrm{aux}}_{ij} u_{i,1} - \sigma_{ik} \varepsilon^{\mathrm{aux}}_{ik} \delta_{1j}) q_{,j} \, \mathrm{d}\Omega + \int_{\Omega} [\sigma_{ij} (u^{\mathrm{aux}}_{i,1j} - \varepsilon^{\mathrm{aux}}_{ij,1})] q \, \mathrm{d}\Omega - \int_{\Omega} (C_{ijkl,1} \varepsilon_{ij} \varepsilon^{\mathrm{aux}}_{kl}) q \, \mathrm{d}\Omega \tag{18}$$

Incompatibility formulation is adopted here to select auxiliary fields for the implementation of interaction energy integral (see details in Ref. [19]). Note that the second integral in Eq. (18) arises from the incompatibility of auxiliary displacement and strain fields in graded composites and the third integral is nonzero due to the property inhomogeneity in 2D-GCs. Once the interaction energy integral is calculated, mode-I and mode-II SIFs can be extracted individually by

$$I = \frac{2}{E^*_{\mathrm{tip}}} (K_{\mathrm{I}} K^{\mathrm{aux}}_{\mathrm{I}} + K_{\mathrm{II}} K^{\mathrm{aux}}_{\mathrm{II}}) \tag{19}$$

$$K_{\mathrm{I}} = \left(\frac{E^*_{\mathrm{tip}}}{2}\right) \cdot I; \; K^{\mathrm{aux}}_{\mathrm{I}} = 1.0, \; K^{\mathrm{aux}}_{\mathrm{II}} = 0.0 \tag{20}$$

$$K_{\mathrm{II}} = \left(\frac{E^*_{\mathrm{tip}}}{2}\right) \cdot I; \; K^{\mathrm{aux}}_{\mathrm{I}} = 0.0, \; K^{\mathrm{aux}}_{\mathrm{II}} = 1.0 \tag{21}$$

where K_{I} and K_{II} are the mode-I and mode-II SIFs; $K_{\mathrm{I}}{}^{\mathrm{aux}}$ and $K^{\mathrm{aux}}_{\mathrm{II}}$ the mode-I and mode-II SIFs of auxiliary fields; E^*_{tip} is the Young's modulus at

crack-tip location which equals to E_{tip} under plane stress condition and $\frac{E_{\text{tip}}}{(1-\nu_{\text{tip}}^2)}$ under plane strain condition.

Based on crack-tip local homogenization hypothesis, the MHS criterion is used here to predict crack growth direction in 2D-GCs. It is assumed that crack propagation occurs in the direction along which the hoop stress reaches its maximum value

$$\left(\frac{\partial \sigma_{\theta\theta}}{\partial \theta}\right)\Bigg|_{\theta=\theta_0}=0,\ \left(\frac{\partial^2 \sigma_{\theta\theta}}{\partial \theta^2}\right)\Bigg|_{\theta=\theta_0}<0 \quad (22)$$

As indicated in previous studies, the crack-tip asymptotic fields in graded composites have the same expressions as ones in homogeneous materials. Therefore, taking the expression of hoop stress $\sigma_{\theta\theta}$ into Eq. (22), one can obtain the crack growth direction in crack-tip local coordinate system as

$$\theta_0=2\arctan\frac{1}{4}\left(\frac{K_{\text{I}}}{K_{\text{II}}}\pm\sqrt{\left(\frac{K_{\text{I}}}{K_{\text{II}}}\right)^2+8}\right) \quad (23)$$

where K_{I} and K_{II} are the mixed-mode SIFs. If $K_{\text{II}}>0$, the crack growth angle $\theta_0<0$, and if $K_{\text{II}}<0$, then $\theta_0>0$. Note that $\theta_0=0$ when $K_{\text{II}}=0$ (pure mode-I crack problem).

In the present simulation, the formulation of interaction energy integral above can be implemented through a simple post-processing step following the graded XFEM calculation, which will produce useful information about the crack propagation in 2D-GCs.

4 Crack Propagation Path Simulation

The whole process of crack propagation simulation in 2D-GCs is divided into three steps: Firstly, establishment of the interaction is developed information between the crack geometry and mesh topology; then, the graded XFEM model is established to calculate stress and displacement fields of cracked 2D-GCs; thirdly, the interaction energy integral post-processing subroutine is executed to determine mixed-mode SIFs and crack growth direction to update the crack geometry. The detailed calculation flowchart is shown in Fig. 5. Note that the crack propagated increment Δa is input as a parameter in advance.

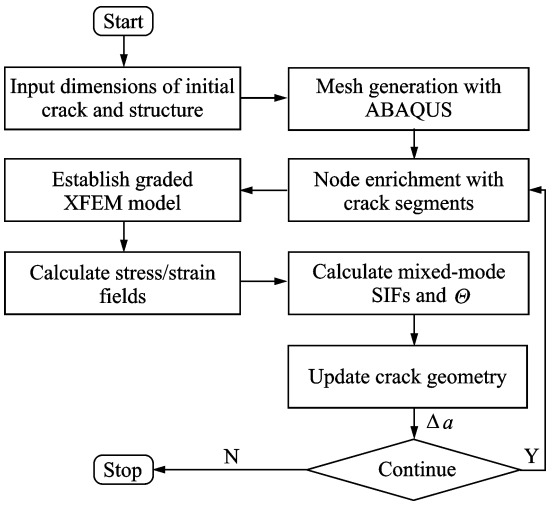

Fig. 5 Calculation flowchart of crack propagation in two-directionally graded composites

5 Numerical Examples and Discussion

In this section, some examples are presented to validate the present graded XFEM to discuss the influences of nonhomogeneous parameters on crack propagations in 2D-GCs.

5.1 Validation of the presented method

Firstly, a single edge notched bending (SENB) beam is adopted to evaluate the crack path simulation capacity of the present method. The geometrical dimensions, loading and constrain conditions and crack configuration are presented in Fig. 6. The detailed calculation parameters are used as: $L=32$ mm, $h=7.2$ mm, $a=2$ mm, $\delta=4$ mm, $P=1$ N, $E=E(y)$, $\nu=\nu(y)$, where a is the crack length, $E(y)$ and $\nu(y)$ are the Young's modulus and the Poisson's ratio which are the same as those in Ref. [20]. Mesh density is the same with that in Ref. [20] as well, which counts out to be 63×24. As shown in Fig. 6, the beam is loaded by an offset force to produce mixed-mode crack growth which has also been experimentally investigated by Jin et al[20]. Fig. 7 presents the crack propagation paths by the present method and Jin et al. [20], respectively. These two crack growth paths are very similar

to each other, which demonstrate the effectiveness and accuracy of the present method.

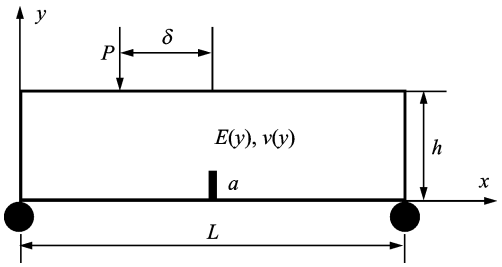

Fig. 6 Single edge notched bending beam with property graded in y direction under offset loading

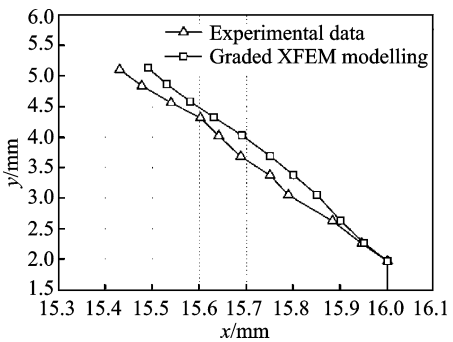

Fig. 7 Comparison of crack propagation paths from the present method and experimental test

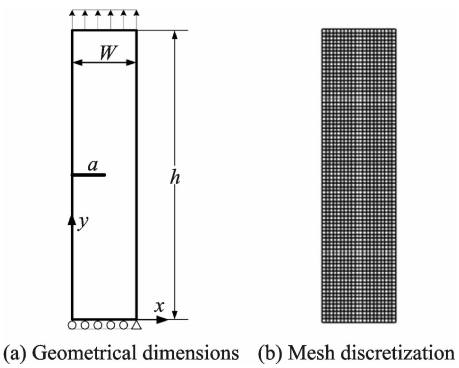

Fig. 8 Single edge notched tension strip under uniform tension

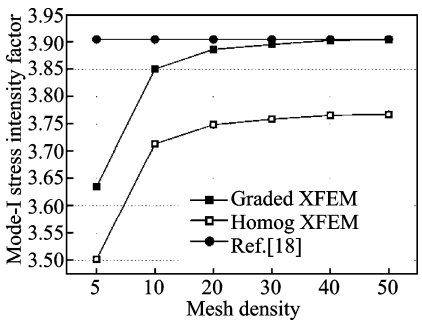

Fig. 9 Mode-I stress intensity factors for graded and homogeneous extended finite element method

Then, a single edge notched tension (SENT) strip is considered to demonstrate the advantage of graded XFEM compared to homogeneous XFEM (element stiffness matrix is calculated by material properties at the central point of element). Its constituent changes from material 1 at the left edge to material 2 at the right edge, as shown in Fig. 8. The calculation parameters are used as: $h/W = 10$, $a/W = 0.50$, $\sigma_t = 1.0$, $E_1 = 3.0$, $v_1 = 0.2$; $E_2 = 1.0$, $v_2 = 0.333$. This example has been investigated by Kim and Paulino[19] which is adopted here as reference. In the calculation, the finite element model is discretized into 4-node rectangular elements (as shown in Fig. 8) and six different mesh densities: 5×50, 10×100, 20×200, 30×300, 40×400 and 50×500 are used. The mode-I SIF calculated by graded, homogeneous XFEM and Ref. [19] are all given in Fig. 9.

As shown in Fig. 9, the convergence rates of graded and homogeneous elements are almost the same, but the result of graded XFEM can converge to the exact solution finally. Obviously, the numerical deviation of homogeneous elements is originated from the property homogenization approximation at the element scale in 2D-GCs and it cannot be eliminated as increasing the mesh density. As validated in Ref. [18], for uncracked graded structures, the stress field calculated by stepwise graded finite element model (which is constituted by homogeneous elements) can be accurate enough as increasing the mesh density. However, it is not the case for cracked graded structures and the numerical derivation of SIFs cannot be removed by refining the mesh.

5.2 Effects of nonhomogeneous parameters on crack propagations

As shown in Fig. 10, a SENT two-directionally graded plate is used to investigate effects of nonhomogeneous parameters on crack propagations in 2D-GCs. The discussed parameters include m_x and m_y, which describe property varying shapes, and E_2/E_1 and E_3/E_1, which de-

scribe property varying steepness (effects of gradient of Poisson's ratio are not considered here). The finite element model is discretized into 4-node rectangular elements and consists of 1 600 elements and 1 701 nodes. The calculation parameters are specified as: $W=1$ mm, $h/W=4$, $a/W=0.18$, $\sigma=100$ MPa, $v(0.9W, 0.5h)=0$, $u(W, 0.5h)=v(W, 0.5h)=0$. In the process of crack propagation simulation, crack increment at each step is assumed as $\Delta a(\mathrm{SENT})=0.05$ mm.

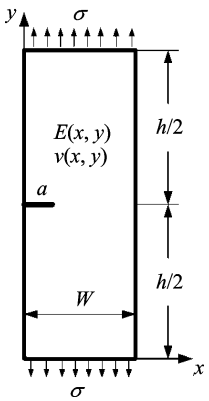

Fig. 10 Geometrical dimensions of two-directionally graded single edge notched tension plate

Effects of parameters m_x and m_y on crack paths are investigated firstly. The 2D-GCs is assumed to be constituted by three components of Al 1100 (constituent 1), Ti-6Al-4V (constituent 2) and SiC (constituent 3), and their mechanical properties are used as: $E_{\mathrm{Al\,1100}}=69$ GPa, $\nu_{\mathrm{Al\,1100}}=0.34$; $E_{\mathrm{Ti\text{-}6Al\text{-}4V}}=115$ GPa, $\nu_{\mathrm{Ti\text{-}6Al\text{-}4V}}=0.293$; $E_{\mathrm{SiC}}=440$ GPa, $\nu_{\mathrm{SiC}}=0.17$. All the discussed parameters include five cases: $m_x=0.2$, $m_y=1.0$; $m_x=5.0$, and $m_y=1.0$; $m_x=1.0$, $m_y=0.2$; $m_x=1.0$, $m_y=5.0$; $m_x=m_y=1.0$. Fig 11 presents the crack growth paths with varying m_x and m_y (only ten crack growth steps are considered in this paper)

In Fig. 11, it is clear that the edge crack is mixed-mode in 2D-GCs under uniform tractions, which is mode-I in homogeneous and traditional x-directionally graded materials. Parameter m_x has no effects on the crack propagation, but the path can be obviously influenced by m_y. When $m_y=0.2$ and $m_y=1.0$, the crack propagation is also mixed-mode and grows towards the bottom

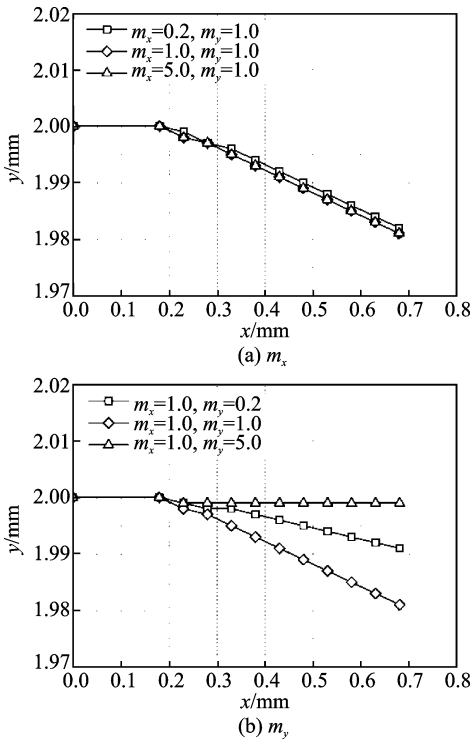

Fig. 11 Crack propagation paths in SENT two-directionally graded plate with various nonhomogeneous parameters m_x and m_y

part of the plate. However, the crack tends to be mode-I and propagates horizontally when $m_y=5.0$. Therefore, it can be concluded that parameter m_x only influences the gradient shape in x direction and thereby having no effects on the propagation of initial x-oriented crack in 2D-GCs, which is reversed for m_y. Furthermore, in the Al 1100/Ti-6Al-4V/SiC material system, Young's modulus at the upper part of the plate is larger than that at the bottom part. So the edge crack propagates in the direction along which Young's modulus decreases gradually (it can be further demonstrated below).

Then, effects of the gradients of Young's modulus in x and y directions are investigated. In the calculation, constituent 1 (Al 1100) is unchanged and Young's modulus of constituent 2 and 3 are assumed to be varied for different property gradients in x and y directions, respectively. For property gradients in x direction, three cases are discussed: $E_2/E_1=0.2$, 1.0, 5.0; and for property gradients in y direction, three cases are investigated: $E_3/E_1=0.2$, 1.0, 5.0. Poisson's

ratios of constituent 2 and 3 are also unchanged and parameters m_x and m_y are always specified as $m_x = m_y = 1.0$. All the crack propagations are shown in Fig. 12.

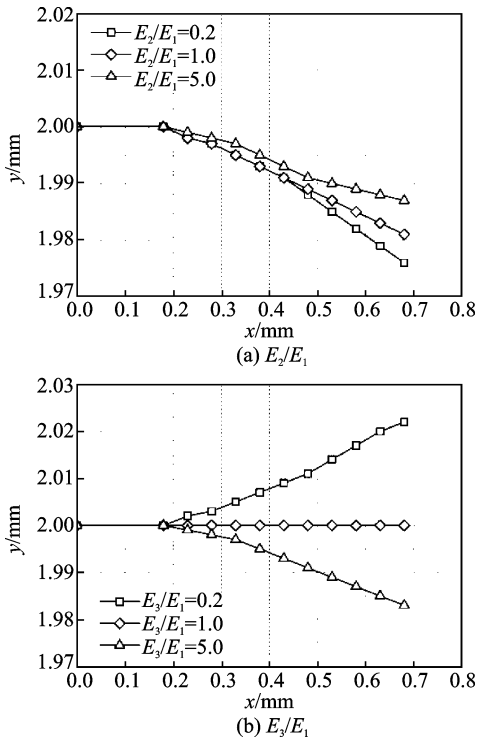

Fig. 12 Crack propagation paths in SENT two-directionally graded plate with various Young's modulus gradients

It is shown that the edge crack propagates to the bottom part in the decreasing direction of effective Young's modulus. Parameter E_2/E_1 has minor effects on the crack path and the crack kink angle declines as E_2/E_1 increasing. It can be explained as: Young's modulus of constituent 2 ascends as E_2/E_1 increasing, which increases the effective Young's modulus of the bottom part and thereby decreases the crack kink angle. The crack paths are considerably influenced by E_3/E_1 which describes the gradient steepness of Young's modulus in y direction. When $E_3/E_1 = 0.2$, the effective Young's modulus at the upper part is smaller and thereby inducing the crack to propagate there. The crack is mode-I and propagates horizontally when $E_3/E_1 = 1.0$ and grows towards the bottom part when $E_3/E_1 = 5.0$. Therefore, the crack always propagates in the declining direction of effective Young's modulus.

To be summarized, for an initial x-oriented edge crack in 2D-GCs, the crack propagation path is obviously affected by property varying shape and steepness in y direction (m_y and E_3/E_1). The crack propagates in the decreasing direction of effective Young's modulus. Specifically, the edge crack becomes to be mode-I and propagates horizontally when $E_3/E_1 = 1.0$.

5.3 Crack propagations in different graded structures

In this example, some cracked structures are designed to investigate crack propagation characteristics in 2D-GCs compared to homogeneous and conventional one-directionally graded materials. All the cracks are mixed-mode induced by offset loading, offset crack and unsymmetric structure, respectively. As shown in Fig. 13, the discussed structures are three-point bending (TPB) under offset loading, four-point bending (FPB) with offset crack and cantilever beam (CB) with unilateral multi-holes. The detailed calculation parameters are as follows:

TPB: $h = 1$ mm, $L/h = 3$, $\delta/h = 0.5$, $a/h = 0.25$, $P = 1$ kN, $u_2(0,0) = 0$, $u_1(L,0) = u_2(L,0) = 0$

FPB: $h = 1$ mm, $L/h = 3$, $\delta/h = 0.25$, $\beta/h = 0.5$, $a/h = 0.25$, $P = 1$ kN, $u_2(0,0) = 0$, $u_1(L,0) = u_2(L,0) = 0$

CB: $h = 1$ mm, $L/h = 3$, $\delta/h = 0.48$, $\beta/h = 1.26$, $\rho/h = 0.78$, $\gamma/h = 0.24$, $r/h = 0.06$, $a/h = 0.8$, $P = 1$ kN, $(u_1, u_2)(x = L) = 0$.

The material system is also constituted by Al 1100, Ti-6Al-4V and SiC. The homogeneous and two-directionally graded material systems are realized by specifying $m_x = 0.0$, $m_y = 0.0$ and $m_x = 1.0$, $m_y = 1.0$, respectively. Nonhomogeneous materials graded in x and y directions are introduced by defining $m_x = 1.0$, $m_y = 1.0 \times 10^6$ and $m_x = 0.0$, $m_y = 1.0$, respectively. The effective Young's modulus and Poisson's ratio are calculated by Eqs. (4)—(6).

MHS criterion assumes that mixed-mode cracks will always propagate in the direction where $K_{II} = 0$ (local symmetry assumption) once

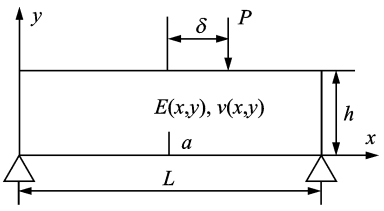

(a) Three-point bending with offset loading

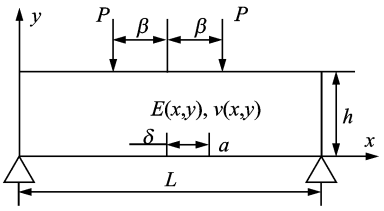

(b) Four-point bending with offset crack

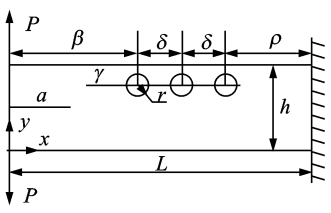

(c) Cantilever beam with unilateral multi-holes

Fig. 13 Geometrical dimensions, loading and constrain conditions of the three cracked structures

they begin to grow, so mode mixity at the initial step has dominant effect on the crack path. Fig. 14(a) gives the mode mixity Φ ($\Phi = \mathrm{arctg}(K_{\mathrm{II}}/K_{\mathrm{I}})$) of the three structures with various nonhomogeneous parameters (material systems) at the first step. For TPB structure, homogeneous and two-directionally graded materials have the largest and the smallest mode mixity, respectively. For FPB structure, mode mixity of one-directionally graded material has the biggest absolute value. And for CB structure, mode mixity of two-directionally graded and homogeneous materials are the largest and the smallest, respectively. Therefore, homogeneous TPB structure and one-directionally graded FPB structure have the largest crack growth angle. For CB structure, two-directionally graded material has the biggest crack growth angle.

Crack propagation paths in the three structures with different material systems are shown in Figs. 14(b—d). As shown in Figs. 14(b, c), for TPB and FPB structures, cracks in different materials have the same growth trend, which validates that offset loading and offset crack dominate the crack propagation compared to material inhomogeneity. Furthermore, crack paths in homogeneous and one-directionally graded materials are almost the same, and crack in two-directionally graded composites has distinct growth path. It is indicated that property gradient in y direction (which is introduced by two-directionally graded material) enhances mode-I deformation of the cracked structure, which makes crack propagate deviating towards vertical direction. In Fig. 14(d), crack paths in homogeneous and grade CB structures are considerably different. For homogeneous material, crack propagates towards the position of hole, which brings premature failure to the cracked CB structure with multi-holes. However, this failure mechanism can be avoided by introducing property inhomogeneity in the CB structure. As validated above, crack in graded composites will always propagate in the decreasing direction of effective Young's modulus. Therefore, the crack propagates deviating to the bottom part that has smaller effective Young's modulus in the cracked CB graded structure (as shown in Fig. 14(d)), which significantly improves its mechanical characteristics. Furthermore, cracks in one-directionally and two-directionally graded CB structures have almost the same propagation paths.

In conclusion, offset loading and offset crack dominate crack growth direction in TPB and FPB structures and property gradient in y direction which is induced by two-directionally graded material makes crack propagate to deviate to the vertical direction. For CB structure with unilateral multi-holes, graded material system can change the crack path and considerably improve mechanical characteristics of the structure.

5.4 Crack propagation by MHS

For graded composites, two property gradients should be considered in crack propagation simulations, and they are the gradients of effective Young's modulus and fracture toughness. Base on the local homogenization hypothesis, the

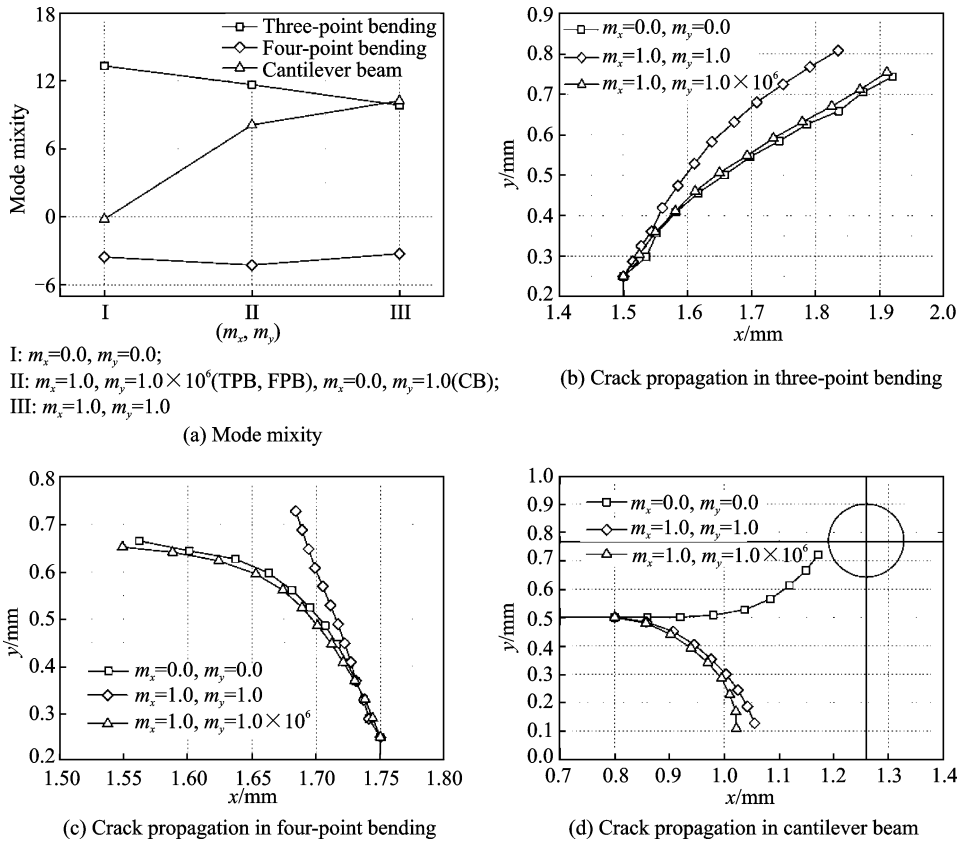

Fig. 14 Mode mixity and crack propagation paths in the three cracked structures with different nonhomogeneous parameters

conventional MHS criterion neglects the effect of fracture toughness gradient. Therefore, in this example, the maximum hoop stress ratio (MHSR) criterion is adopted here to investigate the effect of fracture toughness gradient on crack paths. According to MHSR criterion, crack propagates in the direction along which the MHSR is reached as

$$\left(\frac{\partial \bar{\sigma}_{\theta\theta}}{\partial \theta}\right)\Bigg|_{\theta=\theta_0}=0,\left(\frac{\partial^2 \bar{\sigma}_{\theta\theta}}{\partial \theta^2}\right)\Bigg|_{\theta=\theta_0}<0 \tag{24}$$

$$\bar{\sigma}_{\theta\theta}=\frac{\sigma_{\theta\theta}}{(\sigma_{\theta\theta})_c},(\sigma_{\theta\theta})_c=\frac{K_{IC}(r,\theta)}{\sqrt{2\pi r}} \tag{25}$$

where $\bar{\sigma}_{\theta\theta}$ is the hoop stress ratio; $(\sigma_{\theta\theta})_c$ the critical hoop stress at the crack tip; $K_{IC}(r,\theta)$ the fracture toughness; r the size of fracture process zone. The cantilever beam (CB) with unilateral multi-holes is also adopted here as shown in Fig. 13 and all the calculation parameters are the same as those in section 5.3.

As stated in section 5.3, crack paths in one-directional and two-directional graded CB structures are almost the same. Therefore, y-directionally graded CB structure are employed in the example by setting constitute 1 and 2 as Ti alloy and constitute 3 as ZrO_2. The detailed properties are $E_{Ti}=110$ GPa, $\upsilon_{Ti}=0.33$, $K_{IC,Ti}=60$ MPa·$m^{0.5}$, $E_{ZrO_2}=150$ GPa, $\upsilon_{ZrO_2}=0.25$, $K_{IC,ZrO_2}=2$ MPa·$m^{0.5}$. Fig. 15 shows the crack paths predicted by the MHS and MHSR criterions with various fracture process zone sizes. In Fig. 15 "Ti" is the homogeneous Ti alloy CB structure, "TZ" represents the current constitute configuration of the graded composites and "ZT" the reversed case in which constitute 1 and 2 is ZrO_2 and constitute 3 is Ti alloy. Terms r and a are the sizes of process zone and initial crack, respectively.

As shown in Fig. 15, crack paths by different criterions are obviously dissimilar. For homogeneous Ti alloy CB structure, these two criterions are the same and crack paths are identical to each other. When the size of fracture process zone is set as $r/a=0.01$, crack paths by the MHS and MHSR criterions are almost the same. Crack

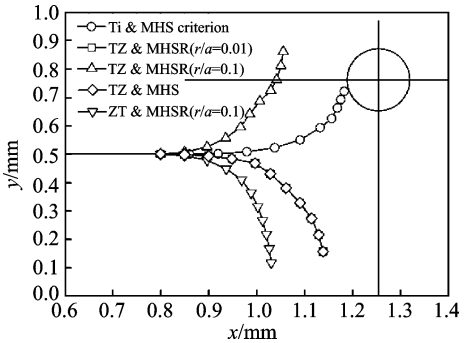

Fig. 15 Crack propagation paths in graded CB structure by the MHS and MHSR criterions with different process zone sizes

propagates towards the region that exhibits smaller Young′s modulus, which demonstrates that Young′s modulus gradient dominates crack propagation and MHS criterion is suitable for crack growth prediction in this case. However, crack path predicted by MHSR criterion with $r/a=0.1$ is absolutely different from that by MHS criterion. Crack propagates in the decreasing direction of effective fracture toughness and MHS criterion cannot be used to simulate crack path. In this situation, the gradient of effective fracture toughness dominates crack propagation. When ZT material system is adopted, crack grows to the bottom region that has smaller fracture toughness according to the MHSR criterion with process size $r/a=0.1$. As stated above, graded composites can be introduced to improve mechanical characteristics of cracked CB structure with unilateral multi-holes by changing the crack path to avoid the pre-existing holes. However, the optimized material design schemes according to MHS and MHSR criterions are absolutely different and fracture process zone size is the crucial influence factor. When MHSR criterion with $r/a=0.01$ and MHS criterion are used, TZ system is the optimized material design scheme. However, when MHSR criterion with $r/a=0.1$ is adopted, ZT material system is better.

Obviously, it can be concluded that there exists an intrinsic length scale λ that dominates crack propagation in graded composites. Crack propagates in the declining direction of effective Young′s modulus when the process zone size is smaller than λ. And crack grows towards the region that exhibits smaller fracture toughness when the process zone size is larger than λ and MHS criterion is not suitable for crack path prediction in this case. That is to say, the local homogenization hypothesis is not reasonable when the fracture process zone size is larger than the intrinsic length scale λ. Fortunately, this conclusion has also been validated through fracture experiments in Ref. [21] in which this intrinsic length scale is named as the intrinsic material gradient length scale which should be tested by accurate fracture experiments for graded composites.

6 Conclusions

Crack propagation paths in two-directionally graded composites (2D-GCs) are investigated in the paper by the finite element method. A graded isoparametric extended finite element method cooperating with interaction energy integral is implemented to calculate mixed-mode stress intensity factors (SIFs) and crack growth direction is predicted by the MHS criterion based on crack-tip local homogenization hypothesis. It is validated that the present method can give relatively accurate predictions of crack propagation paths in 2D-GCs. Nonhomogeneous parameters perpendicular to the crack surface have obvious effects on the crack propagation. Through redesigning material property reasonably, crack growth in graded structure can be changed to improve the mechanical behaviours of cracked structures. The MHS criterion and local homogenization hypothesis at crack-tip are not suitable for crack propagation simulation in graded composites, which provids that fracture process zone size is larger than the intrinsic material gradient length scale.

Acknowledgment

This work was supported by the Fundamental Research Funds for the Central Universities (No. NS2016003).

References:

[1] HEDIA H S, SHABARA M A N, EI-MIDANY T

T, et al. Improved design of cementless hip stems using two-dimensional functionally graded materials [J]. Journal of Biomedical Materials Research Part B: Applied Biomaterials, 2006, 79(1): 42-49.

[2] NEMAT-ALLA M, NODA N. Study of an edge crack problem in a semi-infinite functionally graded medium with two deviensionally nonhomogeneous coefficients of thermal expansion under thermal load [J]. Journal of Thermal Stresses, 1996, 19(9): 863-888.

[3] NEMAT-ALLA M, NODA N. Edge crack problem in a semi-infinite FGM plate with a bi-directional coefficient of thermal expansion under two-dimensional thermal loading[J]. Acta Mechanica, 2000, 144(3/4): 211-229.

[4] NEMAT-ALLA M. Reduction of thermal stresses by developing two-dimensional functionally graded materials[J]. International Journal of Solids and Structures, 2003, 40(26): 7339-7356.

[5] NEMAT-ALLA M, AHMED K I E, HASSAB-ALLAH I. Elastic-plastic analysis of two-dimensional functionally graded materials under thermal loading [J]. International Journal of Solids and Structures, 2009, 46(14): 2774-2786.

[6] NENAT-ALLA M. Reduction of thermal stresses by composition optimization of two-dimensional functionally graded materials[J]. Acta Mechanica, 2009, 208(3/4): 147-161.

[7] ASGARI M, AKHLAGHI M. Transient heat conduction in two-dimensional functionally graded hollow cylinder with finite length[J]. Heat and Mass Transfer, 2009, 45(11): 1383-1392.

[8] ASGARI M, AKHLAGHI M. Transient thermal stresses in two-dimensional functionally graded thick hollow cylinder with finite length[J]. Archive of Applied Mechanics, 2010, 80(4): 353-376.

[9] SAKURAI H. Transient and steady-state heat conduction analysis of two-dimensional functionally graded materials using particle method[C]// Materials Characterisation IV. UK: WIT Press, 2009: 45-54.

[10] ASGARI M, AKHLAGHI M, HOSSEINI S M. Dynamic analysis of two-dimensional functionally graded thick hollow cylinder with finite length under impact loading [J]. Acta Mechanica, 2009, 208(3/4): 163-180.

[11] ASEMI K, SALEHI M, AKHLAGHI M. Elastic solution of a two-dimensional functionally graded thick truncated cone with finite length under hydrostatic combined loads[J]. Acta Mechanica, 2011, 217(1/2): 119-134.

[12] TORSHIZIAN M R, KARGARNOVIN M H, NASIRAI C. Mode III fracture of an arbitrary oriented crack in two dimensional functionally graded material [J]. Mechanics Research Communications, 2011, 38(3): 164-169.

[13] TORSHIZIAN M R, KARGARNOVIN M H. The mixed-mode fracture mechanics analysis of an embedded arbitrary oriented crack in a two-dimensional functionally graded material plate[J]. Archive of Applied Mechanics, 2014, 84(5): 625-637.

[14] CHEN Kang, XU Xiwu, GUO Shuxiang. Stress intensity factors at crack tips in two-directional graded composites[J]. Acta Aeronautica et Astronautica Sinica, 2013, 34(8): 1832-1845. (in Chinese)

[15] REITER T, DVORAK G J, TVERGAARD V. Micromechanical models for graded composite materials [J]. Journal of the Mechanics and Physics of Solids, 1997, 45(8): 1281-1302.

[16] DOLBOW J, BELYTSCHKO T. A finite element method for crack growth without remeshing[J]. International Journal for Numerical Methods in Engineering, 1999, 46(1): 131-150.

[17] SUKUMAR N, PREVOST J H. Modeling quasi-static crack growth with the extended finite element method Part I: Computer implementation[J]. International Journal of Solids and Structures, 2003, 40(26): 7513-7537.

[18] KIM J H, PAULINO G H. Isoparametric graded finite elements for nonhomogeneous isotropic and orthotropic materials[J]. Journal of Applied Mechanics, 2002, 69(4): 502-514.

[19] KIM J H, PAULINO G H. An accurate scheme for mixed-mode fracture analysis of functionally graded materials using the interaction integral and micromechanics models[J]. International Journal for Numerical Methods in Engineering, 2003, 58(10): 1457-1497.

[20] JIN X, WU L, GUO L, et al. Experimental investigation of the mixed-mode crack propagation in ZrO 2/NiCr functionally graded materials[J]. Engineering Fracture Mechanics, 2009, 76(12): 1800-1810.

[21] ABANTO-BUENO J, LAMBROS J. An experimental study of mixed mode crack initiation and growth in functionally graded materials[J]. Experimental Mechanics, 2006, 46(2): 179-196.

Mr. **Zhao Zhenbo** received the B. S. degrees in flight vehicle design and Engineering from Nanjing University of Aeronautics and Astronautics (NUAA), Nanjing, China, in 2011. Now he is a Ph. D candidate of engineering mechanics and focused on damage tolerances of the graded metal materials.

Prof. **Xu Xiwu** received Ph. D. degree in aircraft design from NUAA in 1992. He is a professor of State Key Laboratory of Mechanics and Control of Mechanical Structures and his research is focused on evaluation of structural character of composite material.

Dr. **Guo Shuxiang** received B. S and Ph. D. degree in Physics from NUAA and now he is an assistant professor of College of Aerospace Engineering, NUAA. His research is focused on fracture mechanics of metal materials with multiple cracks.

(Executive Editor: Zhang Bei)